Fluid Dynamics of Oceanic Thermocline Ventilation

JOHN C. MARSHALL AND A. J. GEORGE NURSER

Space and Atmospheric Physics Group, Department of Physics, Imperial College, London, England

ABSTRACT

A flux form of the potential vorticity (PV) equation is applied to study the creation and transport of potential vorticity in an ocean gyre; generalized PV fluxes (**J** vectors) and the associated PV flux lines are used to map the creation, by buoyancy forcing, of PV in the mixed layer and its transport as fluid is subducted through the base of the mixed layer into the thermocline. The PV flux lines can either close on themselves (recirculation) or begin and end on the boundaries (ventilation). Idealized thermocline solutions are diagnosed using **J** vectors, which vividly illustrate the competing process of recirculation through western boundary currents and subduction from the surface.

Potential vorticity flux vectors are then used to quantify the flux of mass passing inviscidly through a surface across which potential vorticity changes discontinuously but at which potential density and velocity are continuous. Such a surface might be the base of the oceanic mixed layer or, in a meteorological context, the tropopause. It is shown that, at any instant, the normal flux of fluid per unit area across such a surface is given, very generally, by

$$S = \mathbf{u} \cdot \mathbf{n} = \frac{[B\boldsymbol{\omega} \cdot \mathbf{n}]}{g\rho[Q]},$$

where **u** is the velocity and **n** is the normal vector to the surface. Here $\boldsymbol{\omega}$ is the absolute vorticity; $B = -gD\sigma/Dt$ is the buoyancy forcing, with D/Dt the substantial derivative and σ the potential density; $Q = -\rho^{-1}\boldsymbol{\omega} \cdot \nabla\sigma$ is the potential vorticity; ρ the in situ density; and g the gravitational acceleration. Square brackets denote the change in the enclosed quantity across the surface.

1. Introduction

The theory of ocean circulation draws heavily on notions of vorticity transport by ocean currents from places where vorticity is imparted by applied torques to favorable dissipation sites. This connection is at its most transparent in classical homogeneous ocean circulation theory based on the absolute vorticity equation. It is reviewed from this perspective by Marshall (1986).

Modern theories of ocean gyres, building on the seminal studies of Rhines and Young (1982) and Luyten et al. (1983), attempt to understand the vertical structure of the gyre. Reviews can be found in Rhines (1986) and Pedlosky (1990). Recent studies have focussed on the role of the mixed layer and its communication with the main thermocline (see Woods 1985; Williams 1989; Nurser and Marshall 1991). Fluid passes between the mixed layer and the thermocline with a definite potential vorticity setting the stratification of the main thermocline beneath. To explain its stratification, we must understand the trans-

port of *potential* vorticity (PV), rather than absolute vorticity, through the gyre.

In the present contribution, a powerful diagnostic framework, based on the flux form of the potential vorticity equation, is set out and applied. It allows the study of potential vorticity changes along isopycnic layers even in the presence of diabatic and mechanical forcing.

We review, in section 2, the general flux form of the potential vorticity equation, first noted by Truesdell (1951) and Obukhov (1962), and its implications as encapsulated in the "generalized potential vorticity flux vector" and "impermeability theorem" introduced by Haynes and McIntyre (1987). They show that the (mass-weighted Ertel) potential vorticity (PV) cannot be transported across any isentropic surface but must be transported along such a surface. It can only be created or destroyed where the surface terminates; in the present oceanic context, this will either be at the ocean's surface or at a solid boundary.

Readers familiar with the foregoing discussion may move directly to section 3 where the formalism is applied, for appropriate thermocline scaling, to consider the creation and transport of potential vorticity through a gyre. We focus attention on ventilated isopycnic layers where PV originates from the ocean's surface. The

Corresponding author address: Dr. John C. Marshall, Earth Sciences Department, Massachusetts Institute of Technology, Building 54, Rm 1526, Cambridge, MA 02139.

flux form provides a great conceptual simplification of the ventilation process. In section 4, the principles involved are illustrated by computing generalized potential vorticity flux vectors (**J** vectors for short) for solutions of the steady thermocline problem due to Marshall and Nurser (1991). Penetrating insights result from the nature of the interaction between the mixed layer and thermocline and the competing processes of ventilation and recirculation.

Finally, in section 5, the diagnostic framework is applied to derive the very general expression quoted in the abstract for the volume flux across a surface at which potential vorticity changes discontinuously. Oceanic (thermocline ventilation) and meteorological (stratosphere–troposphere exchange) applications are mentioned.

2. Generalized potential vorticity flux vectors and the flux form of the potential vorticity equation

Haynes and McIntyre (1987, see also 1990) have set out, following on from the earlier work of Truesdell (1951) and Obukhov (1962), an illuminating view of PV dynamics. It is based on the following conservative flux form of the PV equation, an exact result for a nonhydrostatic fluid:

$$\frac{\partial}{\partial t}(\rho Q) + \nabla \cdot \mathbf{J} = 0 \tag{1a}$$

where

$$\mathbf{J} = \rho Q \mathbf{u} + \mathbf{N}_Q \tag{1b}$$

is a generalized flux of potential vorticity comprising the advective flux $\rho Q \mathbf{u}$ and the nonadvective flux $\mathbf{N}_Q$ defined by

$$\mathbf{N}_Q = -g^{-1} B \omega + \mathbf{F} \times \nabla \sigma. \tag{1c}$$

Here

$$\omega = 2\Omega + \nabla \times \mathbf{u} \tag{2}$$

is the full three-dimensional absolute vorticity, with Ω the angular velocity of the earth;

$$B = -g \frac{D\sigma}{Dt} \tag{3}$$

is the buoyancy forcing, σ the potential density, that is, the density that a parcel of fluid would have if transported adiabatically to some reference pressure;[1]

$$\mathbf{F} = \frac{D\mathbf{u}}{Dt} + 2\Omega \times \mathbf{u} + \nabla p \tag{4}$$

is the viscous or nonconservative body forces per unit mass with ρ the in situ density, and

$$Q = -\frac{1}{\rho} \omega \cdot \nabla \sigma \tag{5}$$

is the potential vorticity.

For oceanographic applications, it is natural to define potential vorticity in terms of potential density rather than potential temperature; signs are consistent with those in Haynes and McIntyre (1987) if it is remembered that θ has been replaced by $-\sigma$ in the definition of Q, Eq. (5).

a. Physical interpretation

Equation (1) is unusual and unfamiliar in as much as terms associated with diabatic and mechanical forcing appear in the definition of a flux rather than as "source" terms. In the more familiar equation for the rate of change of potential vorticity following a particle,

$$\frac{DQ}{Dt} = \frac{1}{g\rho} \omega \cdot \nabla B - \frac{1}{\rho}(\nabla \times \mathbf{F}) \cdot \nabla \sigma, \tag{6}$$

where $D/Dt = \partial/\partial t + \mathbf{u} \cdot \nabla$. There are two terms inducing material tendencies:

1) gradients of buoyancy forcing in the direction of ω that generate stratification in the direction of ω and hence PV and,
2) curls of body forces that lie on surfaces of constant σ.

Noting that $\nabla \cdot \omega = 0$; $\nabla \times \nabla \sigma = 0$, we can rewrite Eq. (6) in terms of the nonadvective flux $\mathbf{N}_Q$, thus

$$\frac{DQ}{Dt} = -\frac{1}{\rho} \nabla \cdot \mathbf{N}_Q.$$

The continuity equation then yields (1a).[2]

It is this reformulation of the tendency terms in Eq. (6) in terms of the divergence of the nonadvective flux $\mathbf{N}_Q$ that permits the flux form (1a) to be written without any source terms, and so take the form of an absolute conservation law in the general "physics" sense.

The terms that make up $\mathbf{N}_Q$ in Eq. (1c) can readily be interpreted physically. Any body-force $\mathbf{F}$ over a limited region spins up (down) fluid to its left (right), thus inducing a sideways transfer of potential vorticity. Likewise, cross-isopycnal mass fluxes driven by buoyancy forcing will, in the presence of vertical shear, bring horizontal momentum upward and downward into the isopycnal sheet, again effecting a transfer of potential vorticity. Examples that serve to illustrate the physical principles involved can be found in Haynes and McIntyre (1987) and McIntyre and Norton (1990).

---

[1] More precisely, σ is the *anomaly* in the potential density. Here we shall refer potential density to atmospheric pressure p_a and define (in the ocean) $\sigma = \rho|_{p=p_a} - 1000$ kg m^{-3}; this appears as σ_θ in the oceanographic literature.

[2] The coefficient of thermal expansion for seawater increases with pressure (see e.g., McDougall 1987), so the solenoidal triple product $\rho^{-1}[\nabla \rho, \nabla p, \nabla \sigma] \neq 0$ at depth and should appear in (6). This implies an additional term in the definition of the nonadvective flux $\mathbf{N}_Q$, (1c).

b. The impermeability theorem

A central result of the work of Haynes and McIntyre (1987) is that there is a simple and very useful restriction on the direction in which net PV transport can take place. They show that σ surfaces *are impermeable to PV even in the presence of buoyancy forcing and frictional forces*—the "impermeability theorem."

By using the identity

$$(\mathbf{u}^{\perp} \cdot \nabla \sigma)\omega^{\perp} + \rho \mathbf{u}^{\perp} Q = 0,$$

where the component of $\mathbf{u}$ perpendicular to the surface of constant σ

$$\mathbf{u}^{\perp} = \frac{\mathbf{u} \cdot \nabla \sigma}{|\nabla \sigma|^2} \nabla \sigma$$

and the corresponding component of ω

$$\omega^{\perp} = \frac{\omega \cdot \nabla \sigma}{|\nabla \sigma|^2} \nabla \sigma$$

to eliminate the $g^{-1}B\omega^{\perp}$ term, McIntyre and Norton (1990) wrote down a form of Eq. (1) that makes the theorem explicit:

$$\mathbf{J} = \rho \mathbf{u}^{\sigma\perp} Q + \rho \mathbf{u}^{\parallel} Q - g^{-1}B\omega^{\parallel} + \mathbf{F} \times \nabla \sigma. \quad (7)$$

Here

$$\mathbf{u}^{\sigma\perp} = -\frac{\partial\sigma/\partial t}{|\nabla\sigma|^2} \nabla\sigma$$

$$\mathbf{u}^{\parallel} = \mathbf{u} - \mathbf{u}^{\perp}$$

$$\omega^{\parallel} = \omega - \omega^{\perp}.$$

The vectors $\mathbf{u}^{\parallel}$ and $\omega^{\parallel}$ are parallel to σ surfaces. The vector $\mathbf{u}^{\sigma\perp}$ is the velocity at which a σ surface moves normal to itself. Thus, the first term in Eq. (7) allows the flux to follow the moving surface, but it cannot pass *through* the surface.

Next we will specialize the very general statement (1) to the oceanic problem, adopting a simple but realistic model of mixed-layer dynamics and thermodynamics overlying an ideal-fluid thermocline.

3. The ventilation of the thermocline from a surface mixed layer

Figure 1 shows a schematic diagram of the subtropical gyre; fluid circulates on isopycnal layers that outcrop into a mixed layer where they are exposed to buoyancy and mechanical forcing. Here the subtropical gyre experiences water-mass transformation, particularly along the deeply convecting outcrop lines on the northern rim of the gyre.

The flux of mass and potential vorticity between the mixed layer and the thermocline is crucial to our understanding of the structure of gyres. It is useful to focus on the budget between isopycnal surfaces comprising fluid between σ and $\sigma + \delta\sigma$, the isopycnal sheet stippled in Fig. 1. The flux form of the potential vor-
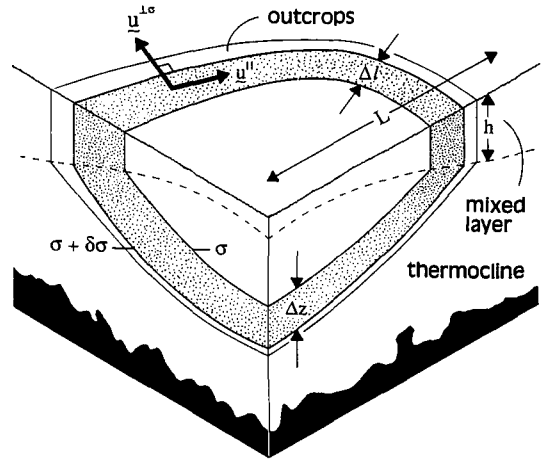

FIG. 1. A schematic diagram showing an isopycnal layer (stippled) outcropping into the mixed layer of a subtropical gyre. The thickness of the layer subtended at the surface is $\Delta\sigma$ in the thermocline Δz. The velocity of a fluid particle in the isopycnal layer is resolved into two components; one component is in the layer, the other perpendicular to it. A typical scale of the gyre is L, a typical mixed-layer depth is h.

ticity equation presented in the previous section provides a very general framework in which to conduct a discussion. The impermeability theorem is of particular utility; it tells us that isopycnal surfaces are impermeable to potential vorticity, even when $\mathbf{F}$ and B are present. As the mixed layer undergoes its seasonal cycle of deepening and shoaling, outcrop lines "march" back and forth. Buoyancy forcing of the mixed layer will drive a flux of *mass* laterally through the vertically inclined isopycnal surfaces. However, because isopycnal surfaces are completely impermeable to potential vorticity, the flux of *potential vorticity* between two isopycnal surfaces must emanate from the free surface or a solid boundary, providing a great conceptual (as well as computational) simplification.

Below, the relative magnitudes of the terms are estimated that make up the generalized PV flux in an isopycnal sheet appropriate to the gyre-scale. Continuity of this PV flux at the base of the mixed layer will lead, in section 5, to quantitative information about the rate of subduction of fluid to and from the mixed layer. A key quantity in our scaling is the ratio of the "mouth" to the "throat" of the isopycnal sheets, defined as follows.

Let the area of an isopycnal sheet exposed at the sea surface be $\Delta l \Delta x$ (the mouth) and the vertical thickness presented by the sheet to the thermocline (the throat) be $\Delta z \Delta x$ (see Fig. 1). Then the ratio of these areas $\Delta z / \Delta l$ is of the same order as the slope of the mixed-layer base or the isopycnal slope, both of $O(h/L)$, so

$$\frac{\Delta z}{\Delta l} \sim \frac{h}{L} \sim \frac{200 \text{ m}}{10^6 \text{ m}} = 2 \times 10^{-4}, \quad (8a)$$

where L is the lateral scale of the gyre (~ 1000 km) and h is a typical mixed-layer depth (~ 200 m).

The other small parameter in our scaling is the Rossby number appropriate to the gyre-scale flow:

$$\text{Ro} = \frac{u}{fL} \sim \frac{10 \text{ cm s}^{-1}}{10^{-4} \text{ s}^{-1} \, 10^6 \text{ m}} = 10^{-3}, \quad (8b)$$

where $u \sim 10$ cm s^{-1} is a typical horizontal flow velocity and $f \sim 10^{-4}$ s^{-1} is the Coriolis parameter. Thus, horizontal currents are closely in geostrophic balance, and the relative vorticity of a fluid parcel is much smaller than the planetary vorticity.

a. Dynamical assumptions

Following Marshall and Nurser (1991), we assume that the isopycnal surfaces that make up the stratified thermocline outcrop "smoothly" (i.e., in a manner consistent with there being no density jump) into a vertically homogeneous mixed layer of variable density σ_m and thickness h. It is supposed that B and $\mathbf{F}$ will only be nonzero in this mixed layer exposed to mechanical forcing by the wind and buoyancy fluxes through the ocean's surface. Our diagnostic framework will accommodate time dependence and take full account of the seasonal march of the surface outcrops and mixed-layer depth.

Mechanical forcing will be confined to a thin surface Ekman layer; below the flow is assumed to be in hydrostatic and geostrophic balance:

$$\left. \begin{array}{c} \mathbf{u}_g = \dfrac{1}{\rho f} \mathbf{k} \times \nabla p \\[2mm] \dfrac{\partial p_m}{\partial z} + \sigma_m g = 0 \end{array} \right\} . \quad (9)$$

The thermodynamic equation within the mixed layer is, from (3),

$$\frac{\partial \sigma_m}{\partial t} + \mathbf{u}_m \cdot \nabla \sigma_m = -B/g,$$

where

$$\mathbf{u}_m = \mathbf{u}_{\text{Ek}} + \mathbf{u}_g + O(\text{Ro}) \quad (10a)$$

is the purely horizontal velocity made up of the Ekman drift

$$\mathbf{u}_{\text{Ek}} = -\frac{1}{\rho f} \mathbf{k} \times \frac{\partial \tau}{\partial z} \quad (10b)$$

(here $\mathbf{k}$ is the unit upward vector and τ the lateral shear stress), $\mathbf{u}_g$ is the geostrophic current, and other ageostrophic contributions, of $O(\text{Ro})$, are neglected.

It is a considerable simplification to partition B into a part, B_{Ek}, associated with Ekman drift across density surfaces; part, B_g, balancing geostrophic advection of density and the density tendency; and a remainder, of $O(\text{Ro})$, associated with other ageostrophic advection:

$$B = B_{\text{Ek}} + B_g \quad (11a)$$

where

$$B_{\text{Ek}} = \frac{g}{\rho f} \mathbf{k} \times \frac{\partial \tau}{\partial z} \cdot \nabla \sigma_m. \quad (11b)$$

Therefore, the thermodynamic equation becomes

$$\frac{\partial \sigma_m}{\partial t} + \mathbf{u}_g \cdot \nabla \sigma_m = -B_g/g. \quad (12)$$

Note that since

$$\frac{\partial}{\partial z} B_g = -g \frac{\partial}{\partial z} \mathbf{u}_g \cdot \nabla \sigma = -g \frac{\partial \mathbf{u}_g}{\partial z} \cdot \nabla \sigma = 0, \quad (13)$$

B_g must be uniform throughout the depth of the mixed layer. This uniformity of the buoyancy-flux convergence allows us to relate B_g to the surface buoyancy influx by integrating (11) through the mixed layer:[3]

$$hB_g + \int_{-h}^0 B_{\text{Ek}} dz + O(\text{Ro}) = \int_{-h}^0 B dz = \mathcal{B}_{\text{in}},$$

where $\mathcal{B}_{\text{in}}$ is the surface buoyancy influx

$$\mathcal{B}_{\text{in}} = g \left(\frac{\alpha_E \mathcal{H}_{\text{in}}}{C_W} - \beta_s \mathcal{S}_{\text{in}} \right), \quad (14a)$$

which includes the heat input per unit surface area $\mathcal{H}_{\text{in}}$ and the salt influx per unit area $\mathcal{S}_{\text{in}}$; α_E is the thermal expansion coefficient; β_s the contraction coefficient for salinity s; and C_W the specific heat of water. Hence,

$$B_g = \frac{\mathcal{B}_{\text{net}}}{h} + O(\text{Ro}), \quad (14b)$$

where the *net* buoyancy flux, the depth integral of that taken up by the geostrophic flow,

$$\mathcal{B}_{\text{net}} = \mathcal{B}_{\text{in}} - \mathcal{B}_{\text{Ek}}, \quad (14c)$$

with

$$\mathcal{B}_{\text{Ek}} = \int_{-h}^0 B_{\text{Ek}} dz = g\mathbf{k} \times \tau \cdot \nabla \sigma_m/(\rho f), \quad (14d)$$

the buoyancy flux taken up into the (vertically integrated) Ekman drift.

b. Potential vorticity flux at the ocean surface

The flux of potential vorticity from the atmosphere into the ocean is of fundamental importance. It is given by the vertical component of $\mathbf{J}$ at the surface of the ocean. Now within the Ekman layer, from Eq. (1b), the vertical component of $\mathbf{J}$ is

$$J_z = \rho Q w - g^{-1} B \omega_z + \frac{1}{\rho} \mathbf{k} \times \frac{\partial \tau}{\partial z} \cdot \nabla \sigma_m, \quad (15)$$

where we have substituted $\mathbf{F} = \rho^{-1} \partial \tau / \partial z$, the body force in the Ekman layer.

---

[3] Since density is continuous at the base of the mixed layer, there are no entrainment fluxes.

The **J** flux upward across the ocean surface, where $w = 0$ (making the rigid lid approximation), is then, using (11) to eliminate the body-force term, simply

$$J_z = -\frac{fB_g}{g} + O(Ro).$$ (16)

Remarkably, the wind-stress forcing does not explicitly appear in Eq. (16), but is implicit in (14) linking B_g to the surface buoyancy influx.

c. Potential vorticity flux in the mixed layer

We avoid an analysis of the **J** field within the Ekman layer, which is sensitive to the detailed turbulent dynamics,[4] by considering the field of **J** in that part of the mixed layer that interacts with the thermocline—the body of the mixed layer, which is forced thermodynamically but not mechanically.

1) VERTICAL COMPONENT

Here $\mathbf{F} \equiv 0$ and $B_{Ek} = 0$, so

$$J_z = \rho Q w - fg^{-1}B_g + O(Ro).$$ (17)

The advective flux of Q is just $\rho Q w$; $-fg^{-1}B_g$ is the nonadvective contribution. In section 3c(3) we will show that $\rho Q w$ is also $O(Ro)$ so that, to $O(Ro)$, J_z is continuous across the Ekman layer.

2) HORIZONTAL COMPONENT

From Eq. (7), the horizontal component of **J** is

$$\mathbf{J} = \rho Q(\mathbf{u}^{\sigma\perp} + \mathbf{u}^{\parallel}) - g^{-1}B\omega^{\parallel},$$ (18)

where $\mathbf{u}^{\parallel}$ and $\omega^{\parallel}$ are components parallel to the contours and $\mathbf{u}^{\sigma\perp}$ is the component of the velocity of the outcrop normal to itself (see Fig. 1). The speed with which the contours march seasonally $|\mathbf{u}^{\sigma\perp}| \sim 2000$ km/6 mo ~ 10 cm s^{-1}, so $|\mathbf{u}^{\sigma\perp}| \geq |\mathbf{u}^{\parallel}|$. This time-dependent part of **J**, which allows the flux to follow the isopycnal surface, is important. It should be emphasized, however, that by the impermeability theorem, even though there will be a flux of mass through the vertically inclined isopycnal surfaces of the mixed layer as occurs when there is diabatic heating, there can be no flux of potential vorticity across isopycnal surfaces.

Furthermore, if the horizontal component of the relative vorticity is evaluated geostrophically using the "thermal wind" equation,

$$\omega_{hg} = \left[-\frac{\partial v_g}{\partial z}, \frac{\partial u_g}{\partial z} \right] = \frac{g}{\rho f} \nabla \sigma_m$$ (19)

we see that $\omega^{\parallel}_{hg} = 0$. Hence, evaluated geostrophically, $\mathbf{J}_h$ is simply

$$\mathbf{J}_h = \rho Q_g^{mix}(\mathbf{u}^{\sigma\perp} + \mathbf{u}_g^{\parallel})$$ (20)

where Q has been replaced by

$$Q_g^{mix} = -\frac{1}{\rho} \omega_{hg} \cdot \nabla \sigma_m = -\frac{g}{\rho^2 f}(\nabla \sigma_m)^2$$ (21)

making use of Eq. (19), and $\mathbf{u}^{\parallel}$ has been replaced by $\mathbf{u}_g^{\parallel}$.

3) SCALING ESTIMATES

Now we estimate the relative magnitude of the terms in the expressions for **J** [Eqs. (17) and (20)]. First consider J_z:

$$\frac{|\rho Q w|}{|fg^{-1}B_g|} \sim \frac{|\rho Q_g^{mix} w|}{f|\mathbf{u}_g||\nabla \sigma_m|} \sim \frac{w}{fh}$$

where h is a typical mixed-layer depth and use has been made of the thermal wind Eq. (19) to estimate $\mathbf{u}_g$ and Eq. (21) to scale Q_g^{mix}.

A very generous upper limit on the mixed layer w is obtained by assuming $w \sim uh/L$, where by (8b),

$$\frac{|\rho Q w|}{|fg^{-1}B_g|} \sim \frac{u}{fL} = Ro \ll 1.$$

We may conclude that the vertical component of **J** is, on the large scale, entirely dominated by the buoyancy forcing term, and so (17) can be replaced by

$$J_z = -fg^{-1}B_g.$$ (22)

How large is the horizontal component of **J**? By (8), the ratio

$$\frac{|\rho Q \mathbf{u}_g^{\parallel}|}{|fg^{-1}B|} \sim \frac{|\rho Q_g^{mix} u|}{f|\mathbf{u}_g||\nabla \sigma_m|} \sim \frac{u}{fh} = \frac{L}{h} Ro \geq 1;$$

so the horizontal and vertical components of **J** are comparable in magnitude.

Thus, for geostrophic scaling the leading terms, horizontal and vertical, of the $\mathbf{J}_g$ flux within the mixed layer are given by

$$\mathbf{J}_g^{mix} = \rho Q_g^{mix}(\mathbf{u}_g^{\sigma\perp} + \mathbf{u}_g^{\parallel}) - fg^{-1}B_g\mathbf{k}.$$ (23)

Note that although the horizontal and vertical terms of $\mathbf{J}_g$ are of the same magnitude, the total vertical flux carried within the mixed layer $\sim L^2 f|g^{-1}B_g|$ and dominates the total horizontal flux $\sim Ro L^2 f|g^{-1}B_g|$ by the large factor $Ro^{-1} \sim 10^3$.

The PV flux from the mixed layer into the thermocline across the base of the mixed layer, which slopes with gradient h/L, is thus completely dominated by the vertical, thermodynamic flux:

$$|J_z| + \frac{h}{L}|J_h| \sim |J_z|(1 + O(Ro)) \sim |fg^{-1}B_g|.$$

This is, to $O(Ro)$, the same flux as is incident across the sea surface [Eq. (16)].

---

[4] It can be shown, however, that for typical oceanic Ekman layer thicknesses, the scaling described below in section 3c(3) remains valid.

The dominating importance of the vertical flux over the horizontal can also be seen by considering flux divergences that induce material tendencies of potential vorticity. Formally the vertical divergence

$$\left|\frac{\partial J_z}{\partial z}\right| \sim \left|\frac{fg^{-1}B_g}{h}\right|$$

dominates the horizontal divergence $|\nabla_h J_h| \sim$ Ro $\times |fg^{-1}B_g/h|$. Within the mixed layer, however, B_g is independent of depth [Eq. (13)], so the leading order of the vertical flux divergence disappears. The balance in the potential vorticity equation must lie between the tendency term, the horizontal divergence, and the vertical divergence of the heating associated with the ageostrophic flow.

d. Potential vorticity flux in the thermocline

Flow in the thermocline is assumed to be free and adiabatic; thus, potential vorticity is conserved following the motion on isopycnal surfaces. The nonadvective flux $N_Q = 0$ and J reduces to the adiabatic flux

$$J^{th} = \rho Q^{th} u = \rho Q_g^{th} u_h + \rho Q_g^{th} w k. \qquad (24)$$

Under normal thermocline scaling,

$$\rho Q_g^{th} = -f \frac{\partial \sigma}{\partial z}. \qquad (25)$$

If this is compared to the PV per unit volume in the mixed layer,

$$\rho Q_g^{mix} \sim -\omega_h \cdot \nabla \sigma_m \sim \frac{u}{h} |\nabla \sigma_m|,$$

it is clear that

$$\left|\frac{Q_g^{th}}{Q_g^{mix}}\right| \sim \frac{1}{\text{Ro}}. \qquad (26)$$

Thus, the horizontal and vertical advective fluxes of Q in the thermocline are greater than the corresponding advective fluxes in the mixed layer by a factor $1/$Ro.
  Hence,

• The vertical advective flux in the thermocline is of the same order as the nonadvective vertical flux in the mixed layer due to buoyancy forcing:

$$|\rho Q_g^{th} w| \sim \frac{1}{\text{Ro}} |\rho Q_g^{mix} w| \sim |fg^{-1}B_g| \sim |J_z^{mix}|.$$

• The horizontal advective flux in the thermocline is a factor L/h larger than the mixed-layer vertical flux:

$$|\rho Q_g^{th} u| \sim \frac{1}{\text{Ro}} |\rho Q_g^{mix} u| \sim \frac{L}{h} |J_z^{mix}|,$$

but the flux carried between two isopycnal surfaces (vertical in the mixed layer; quasihorizontal in the thermocline) is comparable. Both vertical and horizontal Q fluxes in the thermocline are dynamically

significant; vertical and horizontal divergences $|\rho Q_g^{th} w|/h$ and $|\rho Q_g^{th} u|/L$ are both $\sim |J_z^{mix}|/h$.

4. Diagnosis of a steady thermocline model using J flux vectors

Solutions are now diagnosed from the steady thermocline model developed in Marshall and Nurser (1991, hereafter MN), which is a large-scale model appropriate to the Sverdrup interior. A continuously stratified thermocline—③ and ④ in the vertical section of the model (Fig. 2)—is overlain by a vertically homogeneous mixed layer ① and ② of variable depth and density. This mixed layer is exposed to mechanical and thermodynamic forcing. The mixed-layer depth of the model $h(x, y)$ is best interpreted as representing annual maximum (late winter) values.

The thermocline is divided into a motionless abyss ④ and a moving thermocline ③ by the "bowl" $z = -D(x, y)$. Within the moving thermocline, the large-scale potential vorticity $Q = -f\rho^{-1}\partial\sigma/\partial z$ is specified as a function of the Montgomery potential and potential density, even on those isopycnal surfaces that outcrop into the mixed layer. This permits a formulation in which the complete solution, including the structure of the thermocline and the thickness of the mixed layer, depends only on the fields of mixed-layer density and Ekman pumping. Solutions are found by solving the thermodynamic equation for the mixed-layer density by the method of characteristics with the prescribed wind and buoyancy forcing. Purely for simplicity—it is not required by the formulation of the model—the potential vorticity distribution is chosen to be uniform on each isopycnal surface wherever the fluid on that surface is in motion. The reader is referred to MN for precise details of the formulation.

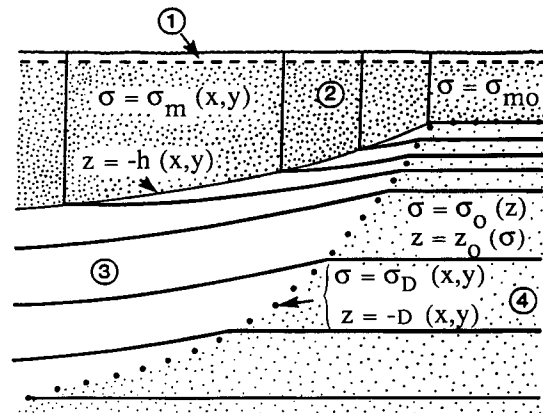The thermocline model has previously been used

FIG. 2. A schematic diagram of the vertical structure of our idealized thermocline model showing ① the shallow Ekman layer, ② the vertically homogeneous mixed-layer of depth $h(x, y)$ and potential density $\sigma_m(x, y)$, and ③ the moving thermocline waters separated by the "bowl" $z = -D(x, y)$ from ④ the resting abyssal fluid with reference stratification $\sigma = \sigma_0(z)$.

(MN) to examine the flow of idealized subtropical and subpolar gyres and in Nurser and Marshall (1991, hereafter NM) to study the entrainment and subduction of fluid into and out of the mixed layer. Here we present and diagnose subduction in a subtropical gyre in terms of J vectors. An idealized pattern of Ekman pumping is used to drive a subtropical gyre in a rectangular basin, which is gently warmed by a surface heat flux so as to induce subduction.

Details. Note that all results have been calculated using full spherical geometry and so are presented in terms of longitude λ and latitude θ. The model subtropical gyre $\lambda_W < \lambda < \lambda_E$; $\theta_S < \theta < \theta_N$, with $\lambda_W = -80°$, $\lambda_E = -20°$; $\theta_S = 15°$, $\theta_N = 40°$ is exposed to the Ekman pumping field:

$$w_e = w_e^* \sin\left[\frac{\pi(\theta - \theta_S)}{\theta_N - \theta_S}\right] \quad (27)$$

with a maximum Ekman pumping $w_e^* = -1.5 \times 10^{-6}$ m s$^{-1} \approx 47$ m yr^{-1}. The pattern of Ekman pumping is plotted in Fig. 3a.

The mixed layer receives a net buoyancy flux,

$$\mathcal{B}_{net} = \frac{g\alpha_E}{C_W}\mathcal{H}_{net} \quad (28a)$$

where the net heating field, plotted in Fig. 3b, is given by

(a)   W$_{EK}$ (m/yr)

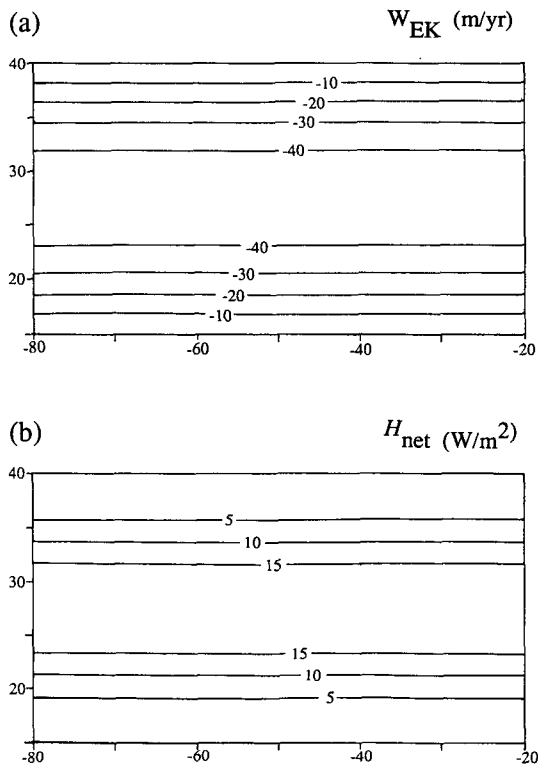(b)   H$_{net}$ (W/m^2)

FIG. 3. The forcing applied to the subtropical gyre. The model subtropical basin extends from 15° to 40°N and from 80° to 20°W: (a) contours of Ekman suction in m yr^{-1}, and (b) contours of net heat input into the mixed layer, in W m^{-2}.

$$\mathcal{H}_{net} = \mathcal{H}_{net}^* \sin^2\left[\frac{\pi(\theta - \theta_S)}{\theta_N - \theta_S}\right]. \quad (28b)$$

The maximum heating rate $\mathcal{H}_{net}^*$ is set to 20 W m^{-2}. Note that $\mathcal{H}_{net} = \mathcal{H}_{in} - \mathcal{H}_{Ek}$ [cf. Eq. (14c)] is the surface heat input less the advection by the Ekman drift. The prescription of $\mathcal{H}_{net}$ is merely for convenience; it is $\mathcal{H}_{net}$ rather than $\mathcal{H}_{in}$ that controls the pattern of subduction.

Vertical structure. The motionless fluid underneath the "bowl" of moving fluid takes up the "reference stratification,"

$$\sigma_0(z) = \begin{cases} 27 - B_L(400 + z), & \text{if } z < -400 \text{ m} \\ 27 - B_U(400 + z), & \text{if } z > -400 \text{ m} \end{cases},$$

where $B_L = 1$ kg m^{-3}/km; $B_U = 3$ kg m^{-3}/km. Within the bowl of moving fluid we specify

$$Q = -f_0\rho^{-1}\frac{\partial\sigma_0}{\partial z},$$

where f_0 is the value of f along the line of zero Ekman pumping on the northern edge of the subtropical gyre. Thus, Q is homogenized to the value possessed by fluid with the reference stratification $\sigma = \sigma_0(z)$ lying on the northern edge of the gyre.

Boundary conditions. The mixed-layer density is specified to increase moving northward along the eastern boundary according to

$$\sigma_m|_{\lambda=20°W} = 26.0 + 0.04 \times (\theta° - 15).$$

No flow, however, is permitted across the eastern boundary within the thermocline; here the bowl coincides with the mixed layer. Thus, by thermal wind, the mixed layer carries a net geostrophic transport into the eastern boundary. This flux is small, totaling 2–3 Sv (Sv $\equiv 10^6$ m^3 s^{-1}) over the whole eastern boundary 15°–40°, compared with the total gyre transport of $\sim$30 Sv. It can be considered to return as an offshore Ekman drift or as an eastern boundary current.

It should be noted that, because the flow is eastward, the above boundary condition is an *outflow* condition; we integrate backward along characteristics. This seems less natural than specifying the inflow, as in MN and NM, but conveniently ensures no flow within the thermocline across the eastern boundary.

A condition is required where the flow is outward through the western boundary, as occurs over the southern half of the boundary; we choose

$$\sigma_m|_{\lambda=80°W} = 26.0 - 0.15 \times (\theta° - 15).$$

This decrease of mixed-layer density moving northward on the western boundary (contrasted with the northward decrease on the eastern boundary) models the increase in temperature toward the west, seen in the subtropical oceans.

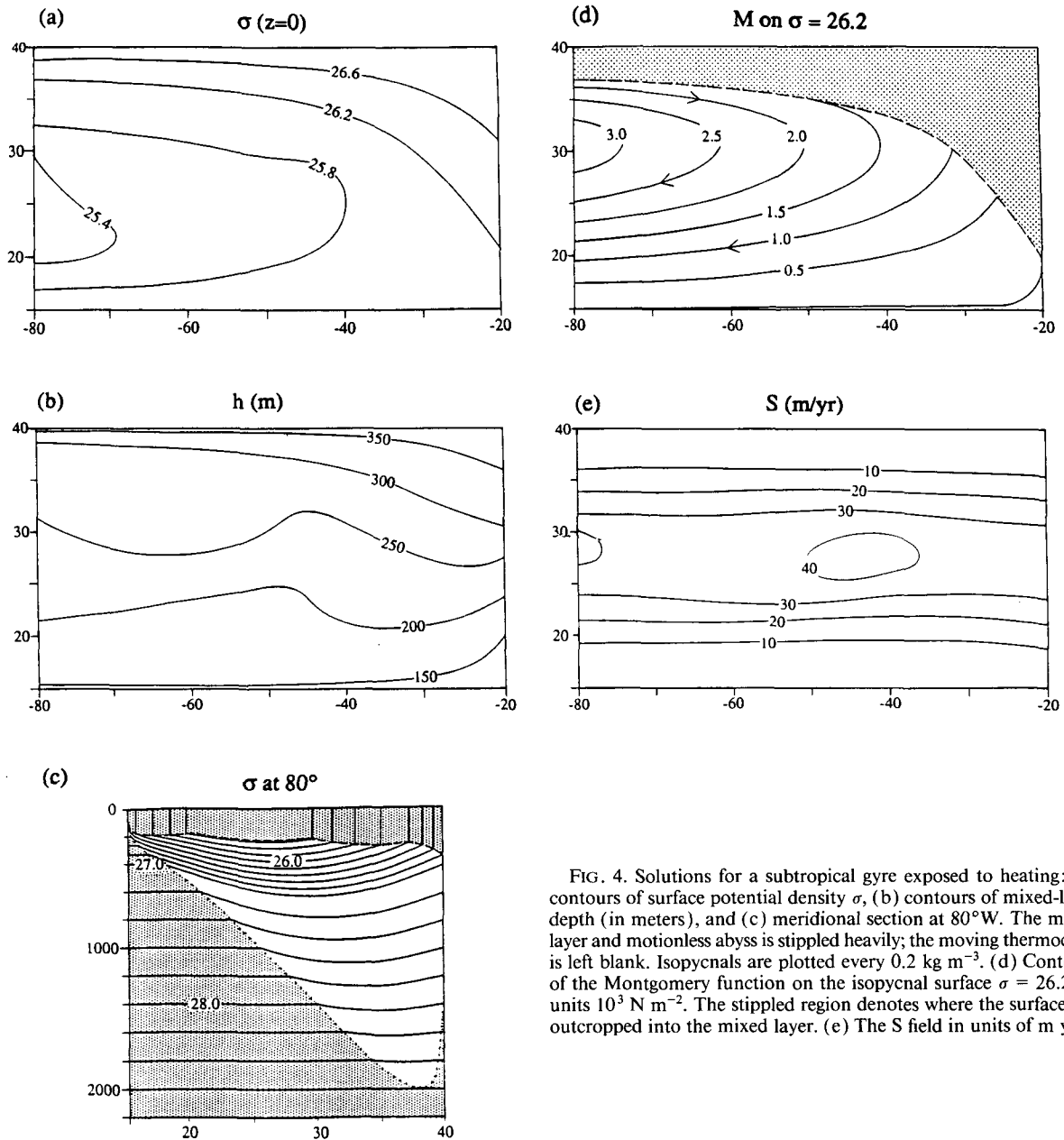*Pattern of flow.* The steady solution is presented in

Fig. 4. Solutions for a subtropical gyre exposed to heating: (a) contours of surface potential density σ, (b) contours of mixed-layer depth (in meters), and (c) meridional section at 80°W. The mixed layer and motionless abyss is stippled heavily; the moving thermocline is left blank. Isopycnals are plotted every 0.2 kg m^{-3}. (d) Contours of the Montgomery function on the isopycnal surface $\sigma = 26.2$, in units 10^3 N m^{-2}. The stippled region denotes where the surface has outcropped into the mixed layer. (e) The S field in units of m yr^{-1}.

Fig. 4. The mixed-layer density contours—the outcrop lines of the isopycnal surfaces (Fig. 4a)—are swept by the clockwise flow around the subtropical gyre with the warmer, lighter water at its center. The mixed-layer depth contours are more zonal, deepening to 400 m on the northern edge of the gyre. The meridional hydrographic section (Fig. 4c) reveals that the vertical structure of the gyre has a pronounced north–south asymmetry with the bowl rapidly deepening to the north. Note how the lighter isopycnal surfaces outcrop into the mixed layer. The near-surface stratification is strong, with weaker stratification below.

The flow on the $\sigma = 26.2$ surface is presented in Fig. 4d. Along the outcrop line fluid is subducted into the thermocline from the mixed layer. It then becomes involved in the clockwise circulation of the gyre and eventually exits into the western boundary current. Much of the fluid to the west, however, is unventilated: it simply recirculates out of, and then back into, the western boundary current without ever passing through the mixed layer. The subduction rate, the rate at which fluid passes from the base of the mixed layer into the thermocline, is plotted in Fig. 4e. In this particular solution it is similar to the Ekman pumping field, Fig.

3a; although, in general, it can be quite different—see the examples given in NM.

a. The flux of potential vorticity between isopycnal surfaces

Fluid parcels in the thermocline of our model, where diabatic forcing is zero, are constrained to follow isopycnal surfaces. It is natural, then, to inquire into the flux of mass and potential vorticity between density surfaces. The prohibition of any PV flux across density surfaces in the mixed layer by the impermeability theorem also suggests the utility of considering the fluxes integrated between density surfaces.

In the mixed-layer isopycnal surfaces are vertical. The total flux carried between outcrops whose (potential) densities differ by $d\sigma$ and therefore lie a horizontal distance $d\sigma/|\nabla\sigma|$ apart is then $|\mathbf{J}^{\text{mix}}|d\sigma/|\nabla\sigma|$ per unit distance along the outcrop (see Fig. 5).

Similarly, the flux carried between these isopycnal surfaces in the thermocline is

$$|\mathbf{J}^{\text{th}}|d\sigma/|\nabla\sigma| \sim \left|\mathbf{J}^{\text{th}}\frac{\partial z}{\partial\sigma}\right|d\sigma$$

per unit distance perpendicular to the direction of $\mathbf{J}^{\text{th}}$ (see Fig. 5). Since $|\mathbf{J}^{\text{th}}| \sim L|J_z^{\text{mix}}|/h$, the magnitudes of these fluxes, $|J_z^m|d\sigma/|\nabla\sigma|$ and $|\mathbf{J}^{\text{th}}\partial z/\partial\sigma|d\sigma$, are similar.
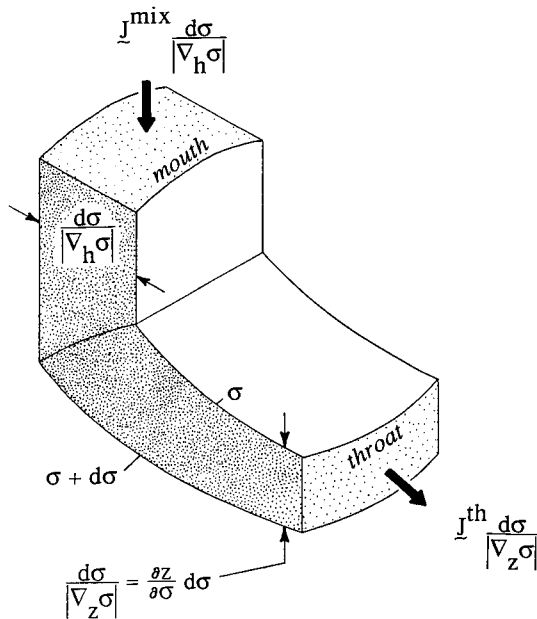

FIG. 5. A schematic diagram defining the mouth and the throat of the isopycnal layer through which the transport of potential vorticity is computed.

We introduce the notation $\mathbf{J}_\mu$ for the flux carried between two isopycnal sheets. In the thermocline the flux of PV between σ and $\sigma + d\sigma$ is given by

$$\mathbf{J}_\mu^{\text{th}} = \frac{\partial z}{\partial\sigma}\mathbf{J}^{\text{th}} = \mu Q^{\text{th}}\mathbf{u}_\sigma$$

where $\mathbf{u}_\sigma$ is the velocity on isopycnal surfaces and $\mu = \rho|\partial z/\partial\sigma|$ is the mass density in σ coordinates. Thus, in the thermocline we plot the vectors

$$\mathbf{J}_\mu^{\text{th}} = \mu Q^{\text{th}}(u_g, v_g, 0) = f(u_g, v_g, 0) \qquad (29)$$

where u_g and v_g are the geostrophic velocities on isopycnal surfaces.

The vanishing of the divergence of this flux in our steady thermocline model is a statement of linear vorticity balance:

$$\nabla_h \cdot \mathbf{J}_\mu^{\text{th}} = \beta v_g + f\nabla_h \cdot \mathbf{v}_g = 0.$$

In the mixed layer,

$$\mathbf{J}_\mu^{\text{mix}} = -\frac{fB_g}{g|\nabla_h\sigma|}\mathbf{k} \qquad (30)$$

is plotted, where B_g is given by Eqs. (14) and (28) and the scaling $1/|\nabla_h\sigma|$ takes account of the spacing between isopycnal surfaces at the sea surface.

We now present $\mathbf{J}_\mu$ vectors in the thermocline $\mathbf{J}_\mu^{\text{th}}$, Eq. (29), and in the mixed-layer $\mathbf{J}_\mu^{\text{mix}}$, Eq. (30), for the thermocline solution described above.

b. J vectors

Figures 6a–c present perspective plots of $\mathbf{J}$ vectors on successively deeper isopycnal sheets, $\sigma = 25.4, 26.2$, and 27.0, in the upper 800 m of the subtropical gyre viewed from the southwest. The $\mathbf{J}$ vectors in the mixed layer point vertically downward; here PV is being created diabatically and flows into the thermocline through the base of the mixed layer. Note that the magnitude of the PV flux—the length of the $\mathbf{J}$ vectors— is set in the mixed layer by the strength of the diabatic processes and continues undiminished into the thermocline; in this steady model, the $\mathbf{J}$ flux is nondivergent. The shallow $\sigma = 25.4$ surface is totally ventilated; all mass and PV is fluxed down from the surface with no recirculation from the western boundary. On the $\sigma = 26.2$ surface, however, both ventilation and recirculation are evident. Here $\mathbf{J}$ vectors emanate both from the western boundary and the mixed layer—ventilation occurs predominantly on the eastern side of the gyre, with recirculation dominating on the west. The deepest layer presented, $\sigma = 27.0$, is completely unventilated. The PV is fluxed in entirely from the western boundary to where it returns after its circuit around the gyre.

It is useful, drawing an analogy from classical E–M theory, to describe the pattern mapped out by the $\mathbf{J}$ vectors as PV flux (or $\mathbf{J}$) lines. They display, in a very pictorial but quantitative way, the complementary
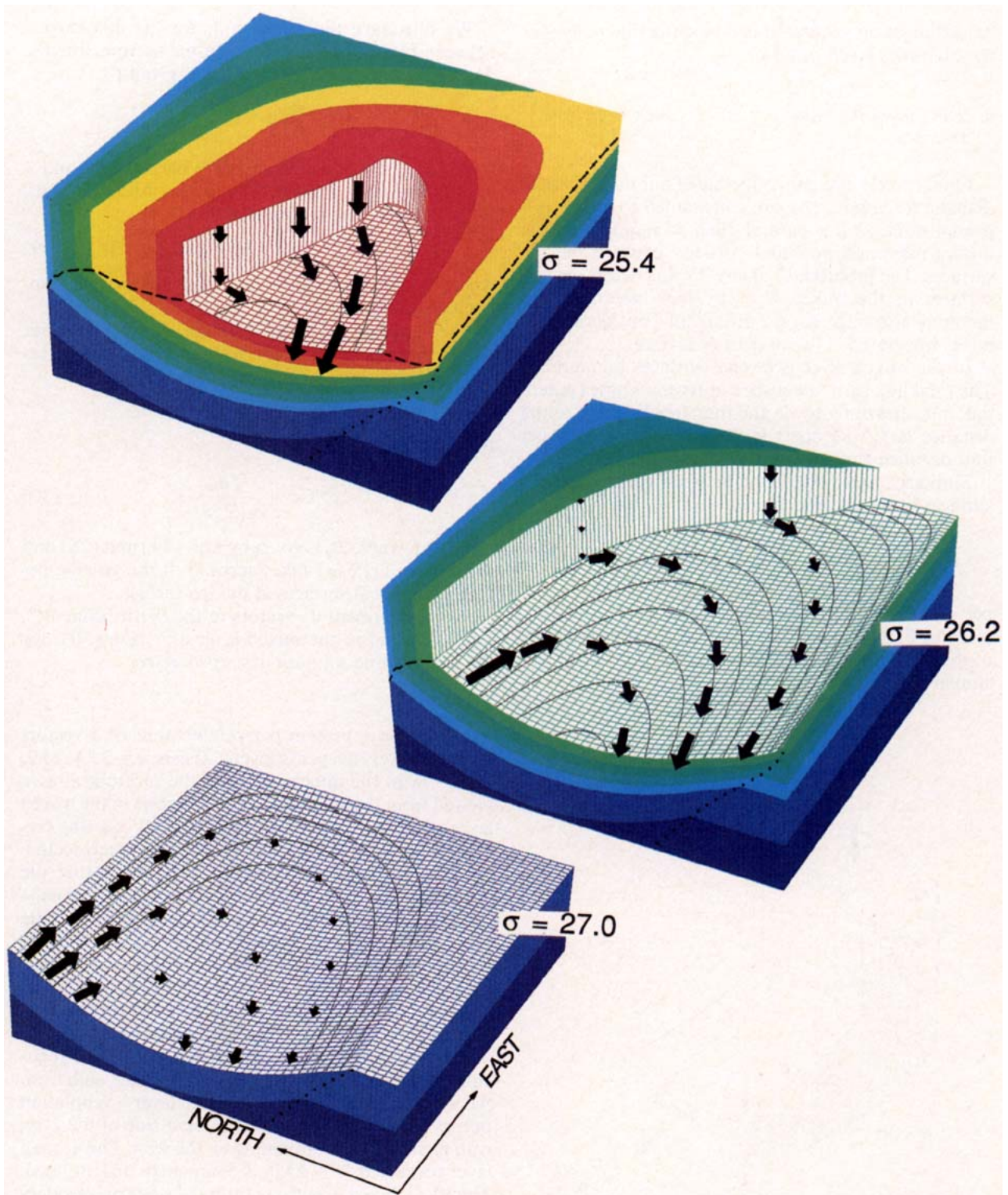
FIG. 6. Perspective plots of the upper 800 m of the subtropical gyre, viewed from the southwest, showing **J** vectors on successively deeper isopycnal surfaces $\sigma = 25.4$, $\sigma = 26.2$, and $\sigma = 27.0$. Each surface appears as a net; its depth is contoured every 25 m. The "wall" denotes where the surface outcrops into the mixed layer. A color scale is used to represent the potential density field, both at the surface and on the vertical planes. Each color covers a density range of 0.1 kg m^{-3}. The mixed-layer base is delineated by a dashed line and the "bowl" by the dotted line.

processes of ventilation and recirculation acting to shape the gyre. They remind us, in particular, of the intimate connection between, on the one hand, ventilation and mixed-layer thermodynamics and, on the other, recirculation and the dynamics of the western boundary current.

It is interesting to revert to a Lagrangian perspective for a moment and consider how the PV of a particle moving out of the mixed layer into the thermocline is changed. Fluid particles in the mixed layer of our model have very small (essentially zero) values of PV. However, at the base of the mixed layer there is a δ-function source on the rhs of the tendency equation, Eq. (6), as the buoyancy forcing B changes discontinuously from a finite value within the mixed layer to zero in the thermocline. It is here, at the base of the mixed layer, that a particle passing through has its PV impulsively set. The flux perspective is unfamiliar but simpler. The $\mathbf{J}$ vector is continuous at the base of the mixed layer,[5] but its manifestation suddenly changes from a nonadvective diabatic flux in the mixed layer to an advective adiabatic flux within the thermocline.

5. Buoyancy-driven mass fluxes: A general statement

Expressions for $\mathbf{J}$ have been written both in the mixed layer and the thermocline under appropriate thermocline scaling. In the presence of buoyancy forcing the $\mathbf{J}$ flux in the mixed layer must have a component directed vertically and thus "communicate" with the thermocline. We now consider in more detail how this flux crosses into the thermocline and derive a very general expression for the subduction rate.

Initially, full generality is retained, and the buoyancy-driven volume flux of an inviscid fluid is computed across any surface at which there is a discontinuity in potential vorticity jumping from Q_1 to Q_2 (see Fig. 7a) but at which potential density and velocity are continuous. Such a surface could be the base of the mixed layer or, in a meteorological context, the tropopause separating stratospheric and tropospheric air. Suppose the "downward" (i.e., inward on the $_1$ side, outward on the $_2$ side) unit normal to the surface under consideration is $\mathbf{n}$.

Let us first assume steady-state conditions. Then the component of $\mathbf{J}$ across the surface is continuous with

$$\mathbf{J}_1 \cdot \mathbf{n} = \mathbf{J}_2 \cdot \mathbf{n}.$$

Velocities are also assumed to be continuous, and furthermore, the flow to be inviscid ($\mathbf{F} \equiv 0$), so

$$\mathbf{J}_1 \cdot \mathbf{n} = \rho Q_1 \mathbf{u} \cdot \mathbf{n} - g^{-1} B_1 \omega_1 \cdot \mathbf{n}$$

$$\mathbf{J}_2 \cdot \mathbf{n} = \rho Q_2 \mathbf{u} \cdot \mathbf{n} - g^{-1} B_2 \omega_2 \cdot \mathbf{n}. \tag{31}$$

Hence, the volume of fluid subducted (i.e., passing from $_1$ to $_2$) per unit area is

---

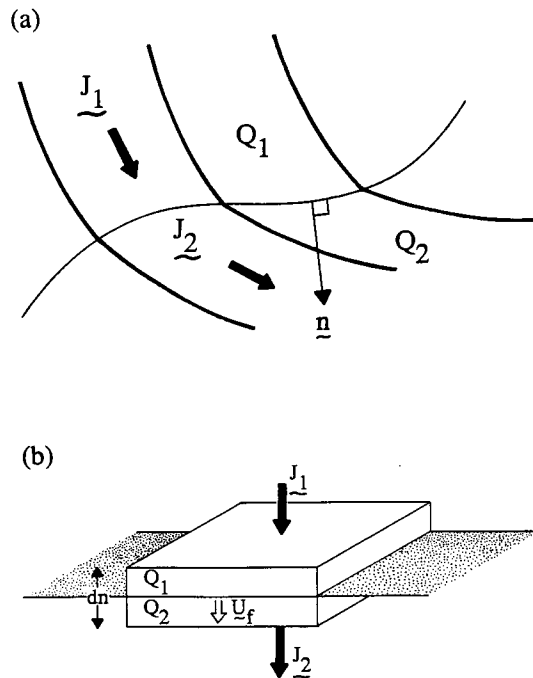[5] This is only true because we have assumed a steady state.

FIG. 7. (a) The transport of volume and the flux of Q is considered across a surface, defined by the unit normal $\mathbf{n}$, at which the potential velocity changes discontinuously. (b) The control volume, fixed in space, through which the surface moves with velocity $\mathbf{u}_f$.

$$S_a = \mathbf{u} \cdot \mathbf{n} = \frac{[B\omega] \cdot \mathbf{n}}{g\rho [Q]}, \tag{32}$$

where the brackets denote the jump $(_1 - _2)$ in the quantity across the surface and the subscript $_a$ denotes per unit area of the surface.

Equation (32) can also be recovered when the surface moves through the fluid if S_a is interpreted as the flux through that moving surface. Consider a control volume fixed in space: a flat pillbox (Fig. 7b) parallel to and surrounding the surface of area dA and thickness dn. The unit normal is again $\mathbf{n}$. Suppose that the surface moves with velocity $\mathbf{u}_f$. Since the surface moves through the pillbox, the pillbox contains regions where Q takes on both values Q_1 and Q_2.

The PV flux equation (1a) yields

$$\frac{\partial}{\partial t} \int \rho Q dA dn = \int \mathbf{J}_1 \cdot \mathbf{n} dA - \int \mathbf{J}_2 \cdot \mathbf{n} dA.$$

Since the change in the total ρQ contained within the pillbox simply reflects the downward propagation of the surface through the control volume, it can be expressed

$$\frac{\partial}{\partial t} \int \rho Q dA = \rho [Q] \mathbf{u}_f \cdot \mathbf{n}.$$

Substituting for $\mathbf{J}_1$ and $\mathbf{J}_2$ from (31), we obtain

$$\rho [Q] \mathbf{u}_f \cdot \mathbf{n} = \rho [Q] \mathbf{u} \cdot \mathbf{n} - g^{-1} [B\omega] \cdot \mathbf{n}.$$

Thus, the rate, S_a, at which fluid is subducted across the moving surface per unit area is

$$S_a = (\mathbf{u} - \mathbf{u}_f) \cdot \mathbf{n} = \frac{[B\omega] \cdot \mathbf{n}}{g\rho[Q]} .$$

Thus, (32) holds for the time-dependent case also. It is an exact statement for inviscid flow.

It is now applied to our thermocline ventilation problem.

Ventilation rates of the oceanic thermocline

Imagine that the surface under consideration is the base of the mixed layer, lying at a depth h below the ocean surface. Within the mixed layer $Q = Q^{mix}$, while in the thermocline $Q = Q^{th}$. The unit downward normal to the mixed-layer base is

$$\mathbf{n} = \frac{-\mathbf{k} - \nabla_h h}{\sqrt{1 + (\nabla_h h)^2}} .$$

The vertical component of $\mathbf{n}$ is $O(1)$ and the horizontal component of $\mathbf{n}$ is of $O(h/L)$. Flow in the thermocline is supposed to be adiabatic, with $B \equiv 0$, while the mixed layer is exposed to buoyancy forcing, so $B \neq 0$. Furthermore, for thermocline scaling, $\omega \approx f\mathbf{k}$ and $Q^{th} \gg Q^{mix}$, and Eq. (32) reduces to the result quoted in NM:

$$S \approx S_a \sim \frac{fB_g}{g\rho Q^{th}} + O(\text{Ro}), \qquad (33)$$

where $S = S_a\sqrt{1 + (\nabla_h h)^2} \approx S_a + O(h^2/L^2)$ is the subduction rate per unit horizontal area and $\mathbf{n}$ has been approximated by $\mathbf{k} + O(h/L)$; B_g is given by Eq. (14).

Equation (33) has been derived (and studied in detail) before (see NM) from a more phenomenological perspective. It is now seen in the context of the generalized potential vorticity theorem; it has been derived here without any reference to the detailed mechanistic considerations presented in NM. The S field for the example run of the thermocline model presented here has been plotted in Fig. 4e, making use of the above formula. It should be compared with the Ekman pumping field (Fig. 3a). A moderate heat flux of $\sim$20 W m^{-2} acting on a mixed layer $\sim$ 100 m thick, at whose base the stratification is 3 kg m^{-3} km^{-1}, can drive a substantial flux of $\sim$40 m yr^{-1}.

6. Discussion

We have applied the formalism of generalized potential vorticity flux vectors to quantify and map the creation and transport of potential vorticity through an ocean gyre. It should be contrasted with the Lagrangian point of view emphasized by Rhines (1986) or, in the ventilation context, Woods (1985). The flux formalism leads to a very general but simple statement relating the subduction rate at any instant to the buoy-
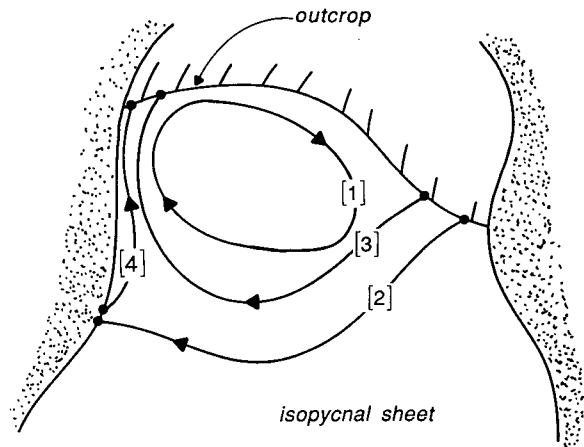

FIG. 8. A schematic diagram showing PV flux lines on an isopycnal surface. Closed flux lines [1] recirculate through the western boundary current. Open flux lines [2] and [3] emanate from the sea surface and can either attach themselves onto the coast [2] or return to the ocean surface [3]. Flux line [4] emanates from the coast and terminates from the sea surface.

ancy forcing of the mixed layer and the jump in potential vorticity across its base. The perspective provided by $\mathbf{J}$ vectors emphasizes the role of the buoyancy, as opposed to mechanical forcing of the mixed layer in controlling subduction and setting the potential vorticity of the thermocline. Indeed, it can readily be seen that a wind blowing over a vertically homogeneous mixed layer can generate only *potential* vorticity there associated with the very weak *horizontal* gradients of density; $Q^{mix} \ll Q^{th}$. The PV of fluid as it crosses the base of the mixed layer into the thermocline is set impulsively by the sharp change in buoyancy forcing. The simplification provided by the use of generalized PV flux vectors, $\mathbf{J}$, however, is that $\mathbf{J}$ is *continuous* at the base of the mixed layer, merely changing from a diabatic nonadvective flux to an adiabatic, advective flux.

Potential vorticity flux lines can either close on themselves or begin and end at boundaries (either free surface or solid), as illustrated schematically in Fig. 8. The closed flux lines [1] in the figure recirculate through the western boundary current. Open flux lines [2] and [3] emanate from the sea surface where there is net buoyancy forcing. But where do they end? On those isopycnal sheets that abut against a solid boundary (the coast or bottom), flux lines can attach themselves onto that boundary [2]; here frictional processes come into play, and $\mathbf{F} \neq 0$ in Eq. (1c), allowing a flux of Q into the boundary. Otherwise (and the only possibility on those isopycnal sheets that do *not* abut) the flux lines must terminate [3] at the ocean surface where the mixed layer cools. The structure of the western boundary current is of crucial importance in deciding how these open flux lines end. Flux lines can also emanate from western boundary currents [4].

In the idealized thermocline model used here to il-

lustrate our ideas, the western boundary current is not represented. In more complete ocean models, inertial and frictional effects must come into play. The method could be straightforwardly and naturally applied to isopycnal models (for example, Bleck et al. 1989) that include dissipative and inertial dynamics in the western boundary layer, as well as more sophisticated mixed-layer physics. It would be fascinating to diagnose such a model using **J** vectors and flux lines.

Finally, we mention a possible meteorological application of these ideas. The change in stratification between the troposphere and lower stratosphere defines the tropopause. The flux of mass and tracers across this surface must be set by vertical gradients in heating and the jump in potential vorticity, as given by the expression for S in the abstract.

REFERENCES

Bleck, R., P. H. Hanson, D. Hu, and E. B. Kraus, 1989: Mixed layer–thermocline interaction in a three-dimensional isopycnic model. *J. Phys. Oceanogr.,* **19**, 1417–1439.

Haynes, P. H., and McIntyre, M. E., 1987: On the evolution of vorticity and potential vorticity in the presence of diabatic heating and frictional or other forces. *J. Atmos. Sci.,* **44**, 828–841.

——, and ——, 1990: On the conservation and impermeability theorems for potential vorticity. *J. Atmos. Sci.,* **47**, 2021–2031.

Luyten, J. R., J. Pedlosky, and H. Stommel, 1983: The ventilated thermocline. *J. Phys. Oceanogr.,* **13**, 292–309.

Marshall, J. C., 1986: Wind driven ocean circulation theory—steady free flow. *Large-Scale Transport Processes in Oceans and Atmosphere,* J. Willebrand and D. L. T. Anderson, Eds., Reidel, 105–161.

——, and A. J. G. Nurser, 1991: A continuously stratified thermocline model including a mixed layer of variable depth and density. *J. Phys. Oceanogr.,* **21**, 1780–1792.

McDougall, T. S., 1987: Neutral surfaces. *J. Phys. Oceanogr.,* **18**, 1950–1964.

McIntyre, M. E., and W. A. Norton, 1990: Dissipative wave-mean interactions and the transport of vorticity or potential vorticity. *J. Fluid Mech.,* **212**, 403–435.

Nurser, A. J. G., and J. C. Marshall, 1991: On the relationship between subduction rates and diabatic forcing of the mixed layer. *J. Phys. Oceanogr.,* **21**, 1793–1802.

Obukhov, A. M., 1962: On the dynamics of a stratified fluid. *Dokl. Akad. Nauk. SSSR* **145**(6), 1239–1242. [English *Sov. Phys. Dokl.,* **7**, 682–684.]

Pedlosky, J., 1990: The dynamics of the oceanic subtropical gyres. *Science,* **248**, 316–322.

Rhines, P. B., 1986: Lectures on ocean circulation dynamics. *Large-Scale Transport Processes in Oceans and Atmosphere,* J. Willebrand and D. L. T. Anderson, Eds., Reidel, 105–161.

——, and W. R. Young, 1982: A theory of the wind-driven circulation. 1. Mid-ocean gyres. *J. Mar Res.,* **40**, 559–596.

Truesdell, C., 1951: Proof that Ertel's vorticity theorem holds in average for any medium suffering no tangential acceleration on the boundary. *Geof. Pur. Appl.,* **19**, 167–169.

Williams, R. G., 1989: The influence of air-sea interaction on the ventilated thermocline. *J. Phys. Oceanogr.,* **19**, 1255–1267.

Woods, J. D., 1985: Physics of thermocline ventilation. *Coupled Atmosphere–Ocean Models,* J. C. J. Nihoul, Ed., Elsevier.